Title

Anomalous temperature dependence of the magnetic field penetration depth in superconducting UBe13

Permalink

https://escholarship.org/uc/item/8ch8c6fj

Journal

Zeitschrift für Physik B Condensed Matter, 64(2)

ISSN

0722-3277

Authors

Gross, F
Chandrasekhar, BS
Einzel, D
et al.

Publication Date

1986-06-01

DOI

10.1007/bf01303700

Copyright Information

Peer reviewed

Anomalous Temperature Dependence of the Magnetic Field Penetration Depth in Superconducting UBe_{13}

F. Gross, B.S. Chandrasekhar*, D. Einzel, and K. Andres
Walther Meissner Institut für Tieftemperaturforschung, Garching,
Federal Republic of Germany

P.J. Hirschfeld
Physik-Department, Technische Universität München, Garching,
Federal Republic of Germany

H.R. Ott
Laboratorium für Festkörperphysik, Eidgenössische Technische Hochschule
Hönggerberg, Zürich, Switzerland

J. Beuers
Max-Planck-Institut für Metallforschung, Stuttgart,
Federal Republic of Germany

Z. Fisk and J.L. Smith
Los Alamos National Laboratory, Los Alamos, New Mexico, USA

We report the first measurements of the magnetic-field penetration depth λ in the heavy electron superconductor UBe_{13}, performed using a SQUID magnetometer. We find the temperature dependence of $\lambda(T) - \lambda(0)$ to follow a T^2 law at low temperatures, giving further evidence of extreme gap anisotropy in this compound. We calculate the temperature dependence expected for a variety of anisotropic states, including those representing certain classes of "exotic" pairing. In general situations, the supercurrent is not parallel to the vector potential, and a more complicated field penetration takes the place of the normal Meissner effect. We argue that the data are consistent with an energy gap with point nodes on the Fermi surface but inconsistent with the large value of the Landau parameter F_1^s expected for a translationally invariant Fermi liquid with large effective mass.

1. Introduction

Something of a stir has been caused by the recent discoveries that, in a number of intermetallic compounds containing either cerium or uranium, the conduction electrons behave as if they had effective masses of tens or, in some cases, hundreds of times

---

* Permanent address: Department of Physics, C.W.R.U., Cleveland, OH 44106, USA

the free electron mass. This behavior has led to the term heavy-electron or heavy-fermion systems. Particular attention has been focussed on some of these materials, like $CeCu_2Si_2$, UBe_{13}, and UPt_3, which are also superconducting. Properties in the superconducting state like the specific heat, critical magnetic fields, ultrasonic attenuation and nuclear spin-lattice relaxation time have been measured [1–7]. Theoretical interpretations fall into two groups: one which leads to $S=0$, $L=0$ Cooper pairs anal-

ogous to normal BCS superconductors, and the other which leads to the possibility of exotic or higher orbital angular momentum pairing with $S=0$ or 1 [2].

If one thinks of a two-fluid description of the superconducting state, one notices that properties like the specific heat, ultrasonic attenuation, and spin-lattice relaxation are determined by the normal fluid. It seemed to us to be of intrinsic interest, as well as complementary to such measurements, to look at a property which is essentially determined by the superfluid component. One such is the persistent supercurrent, or equivalently the penetration depth λ of an external magnetic field. A look at the London expression for this penetration depth

$$\lambda_L = \left(\frac{m^* c^2}{4\pi n_s e^2}\right)^{1/2} \tag{1.1}$$

where m^* is the electron effective mass and n_s is the particle number density of the superconducting electrons, suggests that a measurement of $\lambda(T)$ should give information about m^* and $n_s(T)$. Possible deviations of the latter from the predictions of BCS theory are particularly interesting in the light of other experiments whose non-BCS temperature dependence has been attributed to large gap anisotropy [2-6]. In addition, one sees from the London relation between the current density and the vector potential that, if there is a band of light electrons which are also superconducting, m^*/n_s in (1.1) will be replaced by $[(n_{sh}/m_h^*)+(n_{sl}/m_l^*)]^{-1}$ (h=heavy and l=light), so that a relatively low concentration of light electrons would dominate λ_L. The existence of such a light band has been proposed by Alekseevskii et al. to explain their Hall effect measurements in UBe$_{13}$ [8]. The presence of such light electrons, on the other hand, would hardly affect the normal fluid properties as determined by the other measurements mentioned above. Finally, a measurement of $\lambda(T)$ may reveal [9] whether Fermi liquid effects are important. We defer a discussion of the theoretical details to Sects. 3 and 4.

The plan of the paper is as follows: in Sect. 2 we describe the experimental details and results. In Sect. 3, we calculate the temperature dependence of the London penetration depth for a highly anisotropic order parameter, and compare experiment and theory in Sect. 4. In Sect. 5 we present our conclusions and suggestions for further work.

2. Experimental Method

We first outline the principle of the method, leaving the details for later. The sample is placed in a con-

stant magnetic field less than H_{c1}, inside a pick up coil. Changes of its magnetic moment due to the varying field penetration with temperature are then monitored with a SQUID circuit. Note that this measurement directly yields the changes in penetration depth λ with temperature, but not its absolute value. Now the temperature variation of λ can in general be written as $\lambda(T)=\lambda(0)f(T)$, with $f(0)=1$ and $f(1)=\infty$, so that we can also write $\lambda(T)-\lambda(T_{min})$ $=\lambda(0)[f(T)-f(T_{min})]$. Therefore, if the measured change in the penetration depth $\lambda(T)-\lambda(T_{min})$ can be fitted to a particular function $f(T)$, the absolute value of $\lambda(0)$ may be obtained. The actual form of $f(T)$ may be calculated for any set of assumptions concerning the superconducting state, and in particular the gap anisotropy.

a) Samples

Four samples, prepared by arc-melting the constituents, were studied. Some of their characteristics are shown in Table 1. It will be noted that the densities are lower than the value of 4.41 gm/cm^3 obtained from the lattice parameter of 10.26 $\times 10^{-8}$ cm. This is presumably due to the presence of voids which were clearly visible under a low-power microscope, and particularly pronounced in sample number 3 (roughly 20-70 μm in diameter in samples 1, 2 and 4, but 50-200 μm in sample 3.) This feature introduces some uncertainty in defining the volume of the sample which is penetrated by the field, and it may also be partly responsible for the flux-jumping and irreversible behavior which we shall describe below. However, neither of these will affect the basic conclusions we will draw.

b) Measurements

The change in magnetic flux in the sample with a change in temperature was measured using a SQUID magnetometer with a superconducting inductance bridge first described by Andres et al. [10]. A schematic of the symmetric bridge is shown in Fig. 1. The entire bridge is made from niobium wire with niobium connectors, so that it remains superconducting in the temperature range of interest. With the tantalum shield held normal by heating, currents i and i' are induced in the left and right loops of the bridge by passing suitable currents through L_p and $L_{p'}$. Then the tantalum shield is cooled to become superconducting again, thereby magnetically isolating the bridge circuit. The magnetic fluxes Φ and Φ' linking the left and right loops

Table 1. Some characteristics of the samples

Sample number	1	2	3	4
size (mm) and shape	$1.45 \times 1.61 \times 3.92$ brick-shaped, as-received surface	$1.43 \times 1.53 \times 3.79$ same as sample 1 but surfaces polished to mirror-finish	$\sim 4 \times 2.5 \times 0.22$ irregularly shaped thin sheet	$6.75 \times 1.7 \times 1.5$ brick-shaped with polished faces and rounded edges
Density g/cm^3	4.22	4.31	3.8	4.3
Transition temp. (K)[a]	0.83	0.83	0.77	0.86
Width of transition (K)[b]	0.05	0.05	0.09	0.06
Percentage of Meissner Effect at applied field 0.3 Oe[c]	4%	4%	40%	3.5%

[a] Taken as the midpoint between 10% and 90% flux entry during the initial transition while warming the sample in an applied field of 0.3 Oe

[b] Taken as the width in temperature between the 10% and 90% points defined in (a)

[c] The flux excluded on cooling through T_c in an applied field of 0.3 Oe, as a percentage of perfect flux exclusion
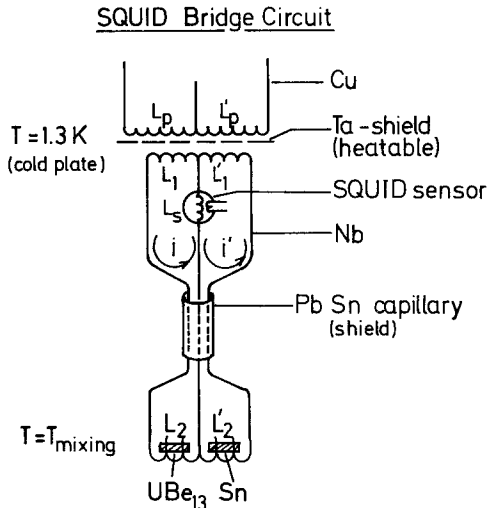
SQUID Bridge Circuit

Fig. 1. A schematic of the superconducting SQUID bridge circuit used for the measurements

are now, respectively $\Phi = (L_1 + L_2)i + L_s(i - i')$ and $\Phi' = (L'_1 + L'_2)i' + L_s(i' - i)$.

A change ΔL_2 of the inductance of the sample coil is produced by a change $\Delta \lambda$ in the penetration depth of the sample resulting from a change ΔT in its temperature. The fluxes Φ and Φ' are, however, separately conserved. Using the approximations for a nearly symmetric bridge $L_1 \approx L'_1$, $L_2 \approx L'_2$, and $i \approx i'$, one can easily see that the resulting change Δi_s in the current through the SQUID is given by

$$\frac{\Delta i_s}{i} = \frac{-L_2}{L_1 + L_2 + 2L_s} \cdot \frac{\Delta L_2}{L_2}. \tag{2.1}$$

In our case the volume V_s of the sample is about 5% of the volume V_2 inside the sample coil, and so one has

$$\frac{\Delta L_2}{L_2} \approx -\frac{\Delta V_s}{V_2}, \tag{2.2}$$

where ΔV_s is the change in that portion of the volume of the sample which is penetrated by the magnetic field, i.e. $\Delta V_s = A \cdot \Delta \lambda$, where A is the surface area of the sample and $\Delta \lambda$ is the change in the penetration depth. Now the change in output voltage ΔQ_s of the SQUID measuring circuit is proportional to Δi_s, and if Q_{s0} is the change in this output as the sample is warmed from the lowest temperature (completely superconducting) to above T_c (flux fully penetrating), then

$$\frac{\Delta Q_s}{Q_{s0}} = \frac{\Delta V_s}{V_s} = \frac{A \cdot \Delta \lambda}{V_s}, \tag{2.3}$$

from which the change in λ resulting from the change in T can be obtained.

The UBe$_{13}$ sample, and a reference sample of single-crystalline tin, were mounted on a silver holder with plastic spacers. The holder carried a carbon resistance thermometer and a heater, and was attached to the mixing chamber of a dilution refrigerator via a thermal link. The holder was positioned so as to locate the two samples in the centers of the coils L_2, L'_2. Stray magnetic fields along the coil axis were reduced to a value below 5 mOe by means of an external μ-metal shield. We estimate the stray field in the transverse direction to be less than 0.01 Oe. The samples were cooled in zero applied field to the lowest temperature of measurement, 0.062 K. A constant measuring field with a value between 0.03 and 0.3 oersted was then applied by inducing a suitable persistent current in the secondary circuit with the tantalum shield held normal by heating it, and then magnetically isolating the circuit

by letting the shield go superconducting. The change in flux penetrating the sample was now monitored as the temperature was swept, thus giving the change in penetration depth $\lambda(T) - \lambda(T_{min})$.

The tin sample served to check the performance of the system, without making any significant contribution to the flux change below 0.9 K when the UBe_{13} sample is superconducting. The SQUID output representing the change in flux penetration in the tin sample as the temperature is swept between 3.7 K and 2.6 K is shown in Fig. 2. The tin data showed the following features, all expected and confirming the proper functioning of the system: there was a 95% Meissner effect, i.e. 95% of the flux was expelled upon cooling through T_c in constant applied field; the change of flux with change of temperature in the superconducting state was quite reversible; over a wide temperature range below T_c, the "empirical" relation $\lambda(T) - \lambda(T_{min}) = \lambda(0)\,[f_{emp}(T) - f_{emp}(T_{min})]$ holds, where $f_{emp}(T) \equiv [1 - (T/T_c)^4]^{-1/2}$, as shown in Fig. 3. From the slope of this plot we find $\lambda(0) = 460$ Å. This is consistent with an earlier measurement by Tai et al. [see Fig. 2 of Ref. 11].

We now turn to the results for UBe_{13}. A typical recording of SQUID output vs. temperature is shown in Fig. 4. Also shown is the change in output expected from a change in flux of two quanta, $2\Phi_0 \approx 4 \times 10^{-7}$ gauss-cm^2; the great sensitivity of the method is apparent. We note the following features of the curve: (1) In region A, where the sample is being initially warmed from the lowest temperature, flux entry proceeds with increasing λ in smooth segments jointed by discrete flux jumps of magnitude Φ_0 or less. (2) If the sweep is now stopped at some temperature , and the sample is then cycled between this and a lower temperature while holding the ap-
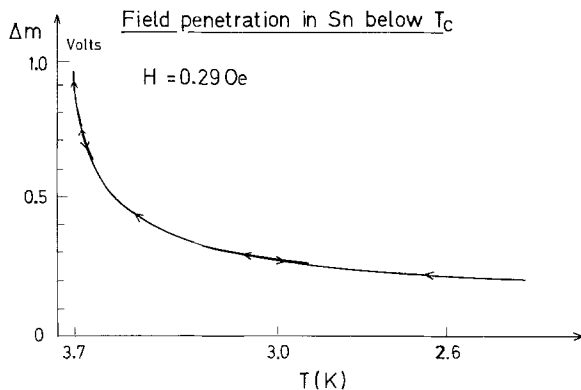
Fig. 3. The incremental penetration depth $\lambda(T) - \lambda(T_{min})$ in tin, evaluated according to (2.3), plotted against the empirical function $f_{emp}(T)$ for a nonlocal superconductor. The slope of the dashed-dotted line corresponds to $\lambda(0) = 460$ Å

Fig. 2. Output signal of the SQUID for the tin reference sample. Note that the T-axis is nonlinear corresponding to the nonlinear characteristic in the carbon thermometer used. The arrows indicate the up and down sweeps in temperature, which are reversible within the experimental uncertainty
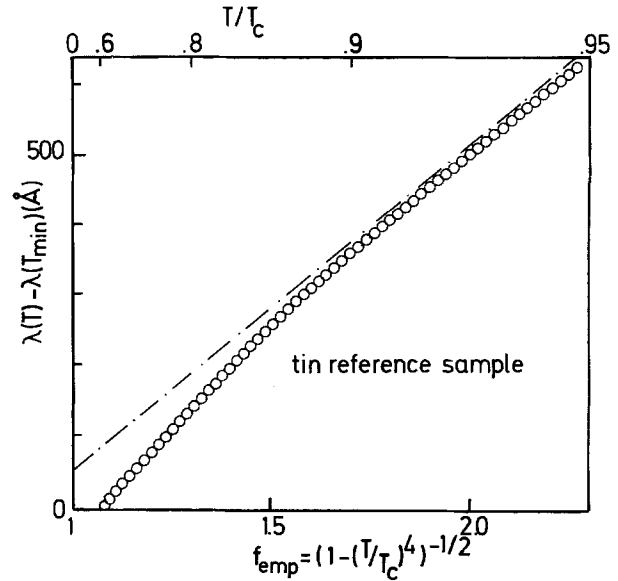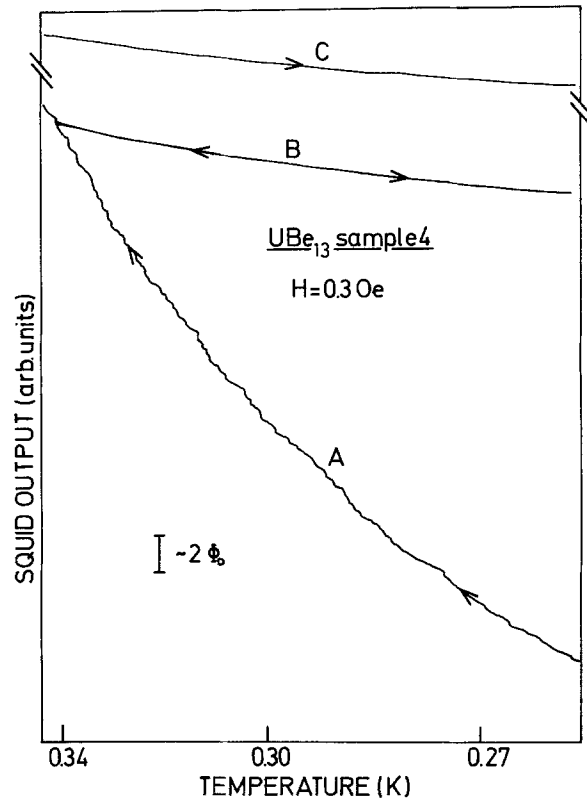
Fig. 4. Observed SQUID output for the UBe_{13} sample number 4 in an applied field of 0.29 Oe. A: initial warmup curve showing both regions of reversible (flatter portions) and irreversible flux entry (steps and steeper portions). B: reversible curve on subsequent cooling and warming back up to same temperature. C: Meissner curve (cooling from above T_c to below T_c; see text)

plied field constant, the change of flux is reversible and without jumps, but an amount of flux Φ_T remains trapped in the sample as shown in region B. (3) If now the applied field is switched off at the lower temperature and then the sample is warmed up to the higher temperature, this trapped flux is ejected from the sample in a way qualitatively similar to the way it entered in region A. (4) The few really smooth sections in region A are nearly parallel to the corresponding reversible sections in region B. In some samples, however, the smooth sections are rather short and are joined by a multitude of very small steps. (5) Finally, if the sample is warmed to above T_c in a constant applied field so that flux entry is complete, and then cooled to the lowest temperature, subsequent temperature cyclings below T_c produce reversible curves (region C) – which we shall call Meissner curves – with slopes almost the same as, but slightly lower than, the corresponding slopes in region B (Fig. 4).

Ideally, irreversible flux trapping would not be expected in measuring fields some 100 times smaller than the lower critical field H_{c1}. In real materials, however, flux trapping always occurs and is due to pinning centers, i.e. inhomogeneities where vortices get trapped and where they can accumulate. Even in low applied fields, in which magnetic vortices would no longer be stable thermodynamically, it is then possible for type II regions to exist in the neighborhood of the pinning centers. This is because the magnetic flux is locally compressed around these centers, such that the local field exceeds H_{c1} and makes the type II state locally stable. Another source for local-field enhancements exists on the sample surface in the form of demagnetizing fields. These fields depend on the shape of the sample and on the surface roughness. They are largest around rough edges, provided the edges are larger in size than the penetration depth. Near such edges, again, the flux can penetrate in the form of type II regions, having the effect of "smoothing out" the sample surface. This effect operates mostly on the geometric edges of the sample, but also near surface irregularities such as the voids mentioned above. Since the samples were mechanically polished, it is possible that the value of H_{c1} on the surface is even lower than that in the bulk, which would enhance this kind of surface flux trapping.

The irreversible observed flux jumps during the initial warmup of the sample are consistent with this model. Flux vortices can penetrate the sample locally, without threading its entire length. This explains why some of the jumps are considerably smaller than what would correspond to a uniform flux change of Φ_0 over the whole length of the sample.

During scanning the Meissner curves, most of the flux remains in the sample due to the pinning centers inside. The demagnetizing fields are much smaller and there is less cause for changing the vortex density in the surface. This is why the remaining observed and reversible flux change in the Meissner state is due to the field penetration at the surface only. The fact that this change is somewhat smaller than that observed in the "reversible" part of the initial warmup curves is explained by the difference in demagnetization factor in the two cases. Since the reversibility of the Meissner curves is near-perfect, we believe that they yield the best measurement of the variation of the penetration depth with temperature, and we therefore use exclusively them for determining $\lambda(T)$.

c) Results

Figure 5 shows data from a typical Meissner, or field-cooled, run using sample 4 (left scale), plotted vs. $(T/T_c)^2$. Also shown, for comparison, are the data from the tin reference sample (right scale). The most striking feature of the UBe₁₃ data is the manifestly good fit to a quadratic temperature dependence over a large temperature range $(0.072 < T/T_c < 0.6)$. Since the absolute scale of the λ axis is unknown, however, we are unable to directly extrapolate the curve to
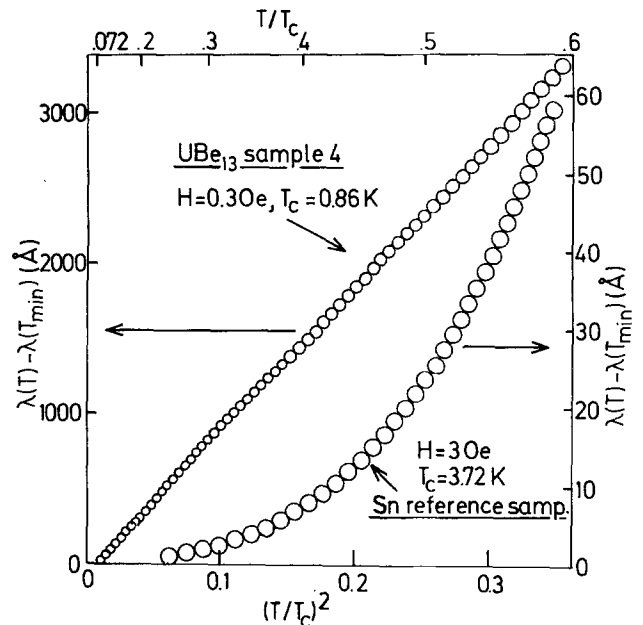

Fig. 5. Incremental penetration depth $\lambda(T) - \lambda(T_{min})$ data, taken from a typical Meissner curve (see text) for the UBe₁₃ sample 4, plotted versus $(T/T_c)^2$ (left scale). The size of the circles shows the measurement uncertainty. Also shown, for comparison, are the data from the Sn reference sample (right scale)

determine $\lambda(0)$. This can only be achieved by a fit to a specific theoretically motivated choice for the function $f(T)$ defined above.

The error bars shown in Fig. 5 (corresponding to the size of the symbols) represent the maximum deviations occuring during different runs on the same sample under identical conditions. These deviations are mainly due to the slow drift of the SQUID output caused by temperature changes in the superconducting circuit.

Other samples showed qualitatively similar reproducible behavior. All exhibited the quadratic temperature dependence, with slightly varying measured slopes which we attribute to errors in measuring the effective surface area, as discussed above.

3. London Kernel and Penetration Depth in Anisotropic Superconductors

In this section we generalize the usual BCS theory for the electromagnetic response of superconductors to systems with anisotropic energy gaps $\Delta(\vec{k})$. We will always neglect non-local contributions to the response kernel since UBe$_{13}$ is well known to be a strongly type II (London) superconductor [7].

Order parameter anisotropy may arise as a consequence of anisotropy in normal state quantities, such as the Fermi velocity or the pairing interaction, or it may be an intrinsic property of an order parameter corresponding to a degenerate representation of the symmetry group of the system. The simplest examples of the latter type of anisotropy are the well-known anisotropic p-wave states of superfluid ^{3}He. Here we calculate the expected electromagnetic response for (1) p-wave states with uniaxial gap anisotropies of the form $\Delta(\vec{k}) = \Delta_0 f(\hat{k} \cdot \hat{l})$, with a symmetry axis $\hat{l}$, and argue that a large class of other anisotropic states, including those consistent with the true symmetry of UBe$_{13}$, will respond similarly at low temperatures. In addition to the model p-wave order parameters, we investigate (2) candidate anisotropic states transforming according to the trivial representation of the crystal point group, i.e. "s-wave-like gaps", and briefly discuss (3) results for gapless superconductors.

a) Penetration Depth in Anisotropic Systems

The electromagnetic response in superconductors can be conveniently discussed in terms of a hydrodynamic two-fluid model. The crystal lattice plays the role of a superleak in neutral superfluids,

clamping the normal electrons and leading to a vanishing normal charge current $\vec{j}^n = 0$. In a steady state situation, the supercurrent takes the well-known hydrodynamic form

$$\vec{j}^s = e \overleftrightarrow{n}^s \vec{v}^s, \tag{3.1}$$

where $\overleftrightarrow{n}^s$ is the superfluid number density tensor and $\vec{v}^s$ the superfluid velocity. If the internal orbital order parameter degrees of freedom are not pinned, there will be additional terms on the right hand side of (3.1), which we neglect for the moment for simplicity. In a charged system $\vec{v}^s$ is given by a term proportional to the gradient of the overall phase φ of the order parameter, and a vector potential contribution:

$$\vec{v}^s = \frac{\hbar}{2m} \vec{\nabla}\varphi - \frac{e}{mc} \vec{A}, \tag{3.2}$$

where m is the mass in the absence of Fermi liquid effects. The explicit form of the phase variation is determined, once the hydrodynamic result (3.1) is known, by simply requiring charge conservation $\vec{\nabla} \cdot \vec{j} = 0$. After Fourier transforming, one finds

$$j_\mu^s \equiv -\frac{e^2}{mc} K_{\mu\nu} A_\nu$$

$$= -\frac{e^2}{mc} \left\{ \overleftrightarrow{n}^s - \frac{(\hat{q} \cdot \overleftrightarrow{n}^s):(\overleftrightarrow{n}^s \cdot \hat{q})}{\hat{q} \cdot \overleftrightarrow{n}^s \cdot \hat{q}} \right\}_{\mu\nu} A_\nu. \tag{3.3}$$

Thus hydrodynamic theory fully determines the linear response function K in the static limit, and allows us to neglect all massive collective modes of the system (for a more detailed discussion, see D. Einzel and P. Hirschfeld, to be published). The linear response of the current to an external vector potential when $\overleftrightarrow{n}^s$ is anisotropic is seen to be qualitatively different from that of an isotropic superconductor, where the inclusion of the second "backflow" term is unnecessary as long as one considers only the transverse part of A. Balian and Werthamer [12] neglected the backflow contribution in their discussion of triplet superconductivity but obtained correct results because they considered only isotropic p-wave states. Recently Millis [13] has derived this term from microscopic theory.

We now turn to the superfluid density n^s, whose full tensor character is realized in the case of superconductors with anisotropic order parameters. In particular, the energy gaps discussed above under (1)–(3) have the common property that they canish on points, lines, or even larger regions of the Fermi surface. As a consequence, the electromagnetic response of the two-fluid system consisting of conden-

sate and thermal excitations (Bogoliubov quasiparticles) is expected to display a temperature dependence qualitatively different from that of an isotropic BCS superconductor. This follows simply because quasiparticles can exist near the zeros of the gap even at extremely low temperatures. The number of such quasiparticles at any temperature is related to the "paramagnetic" part $\vec{n}^p$ of the response kernel:

$$n^p_{\mu\nu} = n \frac{\hbar^2}{m} \sum_k k_\mu k_\nu \left(-\frac{\partial f}{\partial E_k} \right) \equiv n Y_{\mu\nu}(T), \tag{3.4}$$

with $E_{\vec{k}} \equiv \sqrt{\xi^2 + \Delta^2(\vec{k})}$, $\xi \equiv \frac{\hbar^2 k^2}{2m} - \mu$ the quasiparticle spectrum and $f \equiv (\exp E_{\vec{k}}/kT + 1)^{-1}$ the equilibrium quasiparticle Fermi function. The superfluid density tensor $\vec{n}^s$ is then given by the relation $\vec{n}^s = n\vec{1} - \vec{n}^p$. It should be noted that the quantity $\vec{n}^p$ is formally identical to the familiar normal-fluid density tensor only in the case of a translationally invariant system [9].

The presence of zero-energy excitations is reflected in the fact that at low temperatures the paramagnetic response for a state with gap nodes vanishes not exponentially $\sim (2\pi\Delta/kT)^{1/2} \exp(-\Delta/kT)\delta_{\mu\nu}$ as for an isotropic BCS superconductor, but with a power law $\sim (kT/\Delta)^\kappa$. The temperature exponent κ depends not only on the dimension of the manifold of gap nodes (i.e., points, lines, etc.), but also on the rate at which the gap vanishes in the neighborhood of the zeros. We emphasize that power-law temperature dependences will result only if the gap vanishes somewhere on the Fermi surface. An anisotropic gap without nodes will always yield an exponential low-temperature behavior characterized by the minimum value of the gap.

The London penetration depth is now obtained as usual by solving (3.3) subject to the boundary conditions $\vec{h} = \vec{\nabla} \times \vec{A} = \vec{h}_{ext}$, $\hat{z} \cdot \vec{A} = \hat{z} \cdot \vec{j} = 0$ at the surface of the sample defined by normal vector $\hat{z}$. The tensor $n^p_{\mu\nu}$ depends implicitly on the anisotropic order parameter $\Delta(\vec{k})$ through (3.4), while Δ itself is a minimum of the superconducting free-energy functional, which in principle contains all order-parameter orienting effects (except surfaces, which must be included as boundary conditions of the variational problem).

For definiteness, we consider first the special case of a system with spherical Fermi surface and uniaxial order parameter

$$\Delta(\vec{k}) = \Delta_0(T) f(\hat{k} \cdot \hat{l}), \tag{3.5}$$

where $\hat{l}(\vec{r})$ is a local unit axis of gap symmetry and

Δ_0 is the gap maximum. The paramagnetic response (3.4) is then characterized by two eigenvalues corresponding to principal axes parallel and perpendicular to $\hat{l}$:

$$n^p_{\mu\nu} = n^p_\parallel l_\mu l_\nu + n^p_\perp [\delta_{\mu\nu} - l_\mu l_\nu], \quad \text{where}$$

$$n^p_{\parallel,\perp} = 3n \int\limits_0^1 d\cos\vartheta (\cos^2\vartheta, \tfrac{1}{2}\sin^2\vartheta) \int\limits_{-\infty}^\infty d\xi \left(-\frac{\partial f}{\partial E_{\vec{k}}} \right). \tag{3.6}$$

For the moment we ignore competing orienting effects which may tend to bend $\hat{l}$, and consider only spatially homogeneous $\hat{l}$-textures. Substituting (3.6) into (3.3), and assuming transverse gauge $\vec{q} \cdot \vec{A} = 0$, we find a purely transverse current:

$$j_\mu = -\frac{c}{4\pi} \left\{ \frac{1}{\lambda_2^2} \hat{L}_\mu \hat{L}_\nu + \frac{1}{\lambda_1^2} (\delta_{\mu\nu} - \hat{L}_\mu \hat{L}_\nu) \right\} A_\nu \tag{3.7}$$

where $\hat{L}$ is the unit vector associated with the projection of $\hat{l}$ into the $x-y$ plane, and $\lambda_{1,2}$ are the two eigenvalues of the penetration depth tensor

$$\lambda_1^2 \equiv \frac{1}{n^s_\perp} \left(\frac{mc^2}{4\pi e^2} \right),$$

$$\lambda_2^2 \equiv \left(\frac{mc^2}{4\pi e^2} \right) \frac{1}{n^s_\parallel} \frac{n^s_\perp(1 - \hat{l}_z^2) + n^s_\parallel \hat{l}_z^2}{n^s_\perp} \tag{3.8}$$

corresponding to the two directions $\hat{L}$ and $\hat{z} \times \hat{L}$. The result for the field penetration is

$$\vec{h}(z) = \hat{L}(\hat{L} \cdot \vec{h}_{ext}) \exp(-z/\lambda_1)$$
$$+ \hat{z} \times \hat{L}(\hat{z} \times \hat{L} \cdot \vec{h}_{ext}) \exp(-z/\lambda_2). \tag{3.9}$$

For general $\hat{l}$, $\vec{h}(z)$ is seen to rotate in the plane perpendicular to $\hat{z}$ as it penetrates the sample. If $\hat{l}$ is either parallel or perpendicular to $\vec{h}_{ext}$, however, the direction of the field will not change and the penetration is described by a single eigenvalue λ_1 or λ_2.

We further specialize to the polar state $\Delta(\hat{k}) = \Delta_0(T)\,\hat{k} \cdot \hat{l}$, with an equatorial line of nodes, and the axial state $\Delta(\hat{k}) = \Delta_0(T)\,|\hat{l} \times \hat{k}|$, with two point nodes. The latter state is currently believed to represent the high-pressure superfluid A-phase of ^{3}He. In the ^{3}He-A case the axis $\hat{l}$ has the clear physical interpretation of a Cooper pair angular momentum, but in general this need not be true; we emphasize that these two states are simply representatives of two different classes of anisotropic gaps, as discussed below.

The polar and axial states are best characterized by the above-mentioned low-temperature power-law behavior of the paramagnetic response, for which the analytic result is:

$$\lim_{T \to 0} \frac{n^p_{\parallel,\perp}}{n} = \begin{cases} \frac{3}{2}\pi(\ln 2)\left(\frac{kT}{\Delta_0}\right) & \perp \\ \frac{27}{4}\pi\zeta(3)\left(\frac{kT}{\Delta_0}\right)^3 & \parallel \end{cases} \text{Polar} \\ \begin{cases} \frac{7}{15}\pi^4\left(\frac{kT}{\Delta_0}\right)^4 & \perp \\ \pi^2\left(\frac{kT}{\Delta_0}\right)^2 & \parallel \end{cases} \text{Axial} \tag{3.10}$$

It is also instructive to examine the behavior of these curves for the entire temperature range. This may be done numerically using the gap interpolation formula

$$\Delta_0(T) = \delta_{sc} kT_c \tanh\left\{\frac{\pi}{\delta_{sc}}\sqrt{a\left(\frac{\Delta C}{C}\right)\left(\frac{T_c}{T}-1\right)}\right\}, \tag{3.11}$$

where for consistency we insert the weak coupling values of $a=\frac{2}{3}(1,2)$, $\delta_{sc} \equiv \Delta(0)/kT_c = 1.76$ (2.03, 2.46) and the specific heat jump $\Delta C/C = 1.43$ (1.19, 0.78)
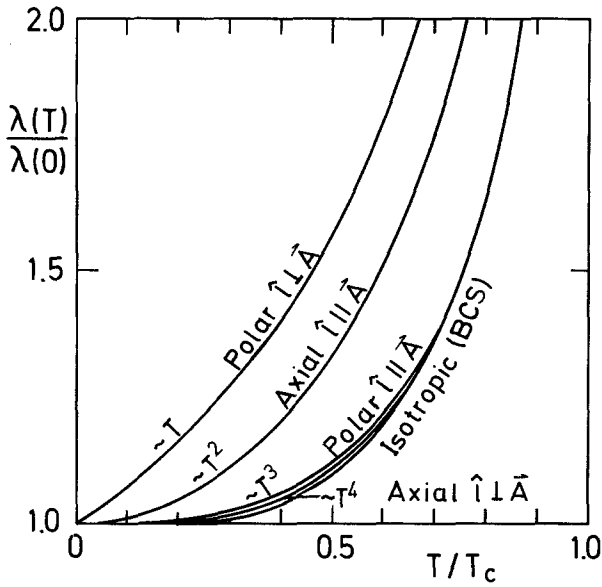

Fig. 6. London penetration depth as a function of reduced temperature T/T_c, for polar, axial and isotropic pairing as given by Eq. (3.12). The temperature dependence of the gap was taken to be of the form (3.11)

for the isotropic (axial [14], polar) state. Since the designations $\parallel$ and $\perp$ refer to $\hat{l}\parallel\vec{A}$ and $\hat{l}\perp\vec{A}$ respectively, we may equally well examine the behaviour of the penetration depths

$$\lambda_{\parallel,\perp} \equiv \left(\frac{mc^2}{4\pi e^2}\right)^{1/2}(n^s_{\parallel,\perp})^{-1/2} \tag{3.12}$$

to which λ_1 and λ_2 reduce for these two $\hat{l}$-textures. In Fig. 6 these are shown alongside the expected BCS-like penetration depth for an isotropic gap.

b) Gap Orientation Effects

It is clear that the predicted penetration depth for a given anisotropic state depends strongly on the direction of the $\hat{l}$-vector, which may be oriented by magnetic fields, superflow, surfaces, or crystal electric fields. As a first approach to this question, we consider the effect of magnetic fields and superflow in the absence of other orienting effects. The relevant contribution to the free energy is

$$F = \frac{1}{2}mv^s_\mu n^s_{\mu\nu}v^s_\nu + \frac{1}{2}h_\mu\chi^s_{\mu\nu}h_\nu, \tag{3.13}$$

where v^s is the superfluid velocity and χ^s is the spin susceptibility. We find the kinetic term to be minimized if $(n^s_\parallel - n^s_\perp)(\hat{l}\cdot\vec{A})^2$ is minimized, while for $\lambda \gg k_F^{-1}$ the spin orientation energy is negligible and will not affect this result regardless of the coupling between the spin and orbital degrees of freedom. From Fig. 6 we see that for the polar (axial) state, $\delta n \equiv n^s_\parallel(T) - n^s_\perp(T)$ is positive (negative) for all temperatures, and that the magnetic coupling tends to align the $\hat{l}$-vector perpendicular (parallel) to the vector potential. The corresponding predictions for the low-temperature penetration depth $\lambda - \lambda(0)$ are therefore a T dependence for the polar state and a T^2 law for the axial state, according to (3.10).

In (3.13) we have neglected the contributions to the free energy which arise from the bending of $\hat{l}$ away from a uniform spatial distribution. These terms stabilize a uniform $\hat{l}$-texture in a bulk neutral system, but in a charged system the coupling of the magnetic field to the order-parameter phase through (3.13) allows for the possibility of a bulk ground state corresponding to nonuniform $\hat{l}$. Dawelbeit [15] has shown that for a bulk ^{3}He-like axial state the Ginzburg-Landau free energy is in fact minimized by a helical texture. Deviations from uniformity are, however, on the order of a few per cent, and we therefore expect that the main effect of magnetic fields and superflow in the bulk is to orient the gap axis as described above.

The orbital terms in the free energy lead to additional terms in the current $\vec{j} = \delta F/\delta\vec{A}$, as mentioned above. For a system with uniaxial anisotropy, these are proportional to $n^s_{\parallel,\perp}$ curl $\hat{l}$ and the backflow term in (3.3) takes on a somewhat more complicated form.

Collisions with the surface will selectively depair certain components of a p-wave order parameter

$\Delta(\vec{k})$ and thereby orient the gap axis $\hat{l}$. Detailed knowledge of the surface scattering processes is needed to draw definitive quantitative conclusions. One expects, however, that the $\hat{l}$-vector in the axial state will be bound perpendicular to the surface if specular scattering dominates [16]. In this case, surface and magnetic effects compete with one another to orient $\hat{l}$. A simple estimate [17] suggests that the effective range of the surface orienting effect in fields of 1 gauss is of the same order of magnitude as the zero-temperature penetration depth; i.e., $\hat{l}$ will bend significantly on this scale, and the solution to (3.3) will inevitably mix $n^s_{\|}$ and $n^s_{\perp}$. At low temperatures, however, the T^2 contribution from $n^s_{\|}$ will continue to dominate the observed $\lambda(T)$.

Finally, we note that crystal electric fields, which are strong in UBe$_{13}$, may also orient the gap, especially in the zero-field limit. In a polycrystalline sample of the type considered here, this effect may give rise to domains in which $\hat{l}$ is roughly spatially homogeneous. Since the three cubic directions are equivalent, however, the system will condense into a state in which the $\hat{l}$-vectors in the various domains will still be roughly aligned with one another. As before, the bending of $\hat{l}$ will cause deviations from the "pure" penetration depths λ defined in (3.12) and depicted in Fig. 6, but at the lowest temperatures the axial state should still display a T^2 law, as opposed to the T law predicted for the polar state.

If the gap axis is strongly pinned by crystal fields, the penetration depth in a single crystal will depend anisotropically on the field direction in the plane of the surface. The simplest situation arises if one can prepare a sample with $\hat{l}$ pointing along one of the axes of a cubic crystal parallel to the surface nearly everywhere. The anisotropy in λ is then given by $(n^s_{\|}/n^s_{\perp})^{1/2}$, which approaches unity at $T=0$ and is maximal at T_c ($\sqrt{3}$ for polar, $\sqrt{2}$ for axial). Unless the experimental geometry is optimally chosen, however, this relatively small effect may be masked by the demagnetizing field. The anisotropy in the rate of increase of λ with temperature, on the other hand, diverges at $T=0$ as $(n^p_{\|}/n^p_{\perp})^{1/2}$, and thus should be easily observable if $\hat{l}$ lies in the plane of the surface.

c) General Considerations; s-Wave-Like Gaps

One may easily generalize many of the above considerations to other anisotropic order parameters, which need not be associated with p-wave pairing. As mentioned above, the temperature exponent κ characterizing the low-temperature behavior of λ and n^p depends on both the set of gap nodes and the rate at which the gap vanishes nearby. For example,

it is easy to see that all gaps $\Delta(\vec{k})$ with point nodes at $\vec{k}_i$ which vanish linearly in $|\vec{k}-\vec{k}_i|$ will quite generally give rise to a T^2 penetration depth at low T, whereas those with *lines* of nodes vanishing linearly will display a T power law. For example, Ohkawa and Fukuyama [18] have proposed a model of extremely local pairing for the heavy fermion superconductors, with an anisotropic gap which transforms according to the trivial representation of the crystal point group ("s-wave-like"):

$$\Delta(k) = \Delta_0(T)\tfrac{1}{3}\{\cos k_x a + \cos k_y a + \cos k_z a\}, \qquad (3.14)$$

where a is the cubic lattice constant. If the Fermi surface anisotropy may be neglected with respect to the anisotropy in the pair potential, the manifold of zeros of $\Delta(\vec{k})$ on the Fermi sphere depends only on the parameter $r \equiv k_F a$. For $(2n+1)(\sqrt{3\pi/2}) \le r \le (2n+3)(\sqrt{3\pi/2})$, the order parameter has lines of nodes circling the fourfold symmetry axes of the cube, and at low temperatures λ is therefore found to vary as T. At the critical values $r_c = (2n+1)(\sqrt{3\pi/2})$ these lines become points, but because the gap now vanishes as $|\vec{k}-\vec{k}_i|^2$, the penetration depth continues to depend linearly on the temperature. For $r < r_c$, one finds an exponential decay, as expected for a gap without nodes.

Similarly, the "s-wave" state proposed by Appel and Overhauser [19], while anisotropic, does not vanish anywhere on the Fermi surface, and therefore gives rise to an exponentially decaying penetration depth at low temperature.

d) Fermi-Liquid Effects

In strongly interacting systems like the heavy-electron superconductors, one expects Fermi-liquid corrections to the above weak-coupling results to be important. These are easily implemented [9] by replacing the tensor $\tilde{n}^s$ introduced above by the renormalized density

$$n^s_{\mu\nu} = \frac{m}{m^*}\left(1 + \frac{F^s_1}{3}Y\right)^{-1}_{\mu\alpha} n\left(1 + \frac{F^s_1}{3}\right)(\delta_{\alpha\nu} - Y_{\alpha\nu}), \qquad (3.15)$$

where $Y_{\mu\nu}$ is the generalized Yoshida function defined in (3.4), m^* is the specific heat mass, and F^s_1 is the $l=1$ spin-symmetric Landau parameter. In a Galilean-invariant system, $m^*/m = 1 + F^s_1/3$, so one might expect F^s_1 to be large in the heavy-electron systems. At $T=0$ the correction to the penetration depth is

$$\lambda = \left(\frac{m^*/m}{1 + F^s_1/3}\right)^{1/2}\lambda_{\text{bare}}. \qquad (3.16)$$

Thus if the large effective mass measured by the specific heat is due mostly to electron-electron interactions, effective mass corrections drop out of the expression for λ at $T=0$ in a translationally invariant system, and should first appear in the leading-order temperature corrections. It is not entirely clear, however, to what extent the Galilean-invariance arguments leading to the effective mass relation should be even approximately valid in a system with localized f-electrons. Valls and Tesanovic [20], Pfitzner and Wölfle [21], and Bedell and Quader [22] have all made use of this relation to discuss the origin of the heavy electron mass. On the other hand, Varma [23] and Rice and Ueda [24] argue that the effective mass should scale with F_0^s instead of F_1^s. It is clear that a measurement of λ can be of considerable use in understanding the nature of the heavy electron ground state.

e) Influence of Impurities

It is well known that nonmagnetic impurities in triplet superconductors would have strong depairing effects similar to those produced by magnetic impurities in ordinary singlet superconductors [12]. Ueda and Rice [25] have recently examined these effects in the s-wave scattering approximation for the case of anisotropic triplet order parameters. Here we follow their approach, a generalization of the usual Abrikosov-Gor'kov theory [26]. Evaluation of the BCS electromagnetic response function in the London limit leads to a simple expression for the "paramagnetic" density tensor:

$$\frac{n_{\mu\nu}^p}{n}=3\frac{\hbar^2}{m}\sum_{k}k_\mu k_\nu (kT)\sum_n \{G(\vec{k},\omega_n)G^*(\vec{k},\omega_n)$$

$$+F(\vec{k},\omega_n)F^+(\vec{k},\omega_n)\}, \qquad (3.17)$$

where F and G are the normal and anomalous Gor'kov functions determined by solving Dyson's equations self-consistently in the presence of the single impurity self-energy

$$\Sigma(\omega_n)=N_i|u|^2\sum_k G(\vec{k},\omega_n), \qquad (3.18)$$

where N_i is the impurity density and u the s-wave scattering matrix element. The corresponding anomalous self-energy vanishes because of the odd parity of the order parameter, and consequently the Green's functions are simply those of the pure system evaluated at renormalized frequency $\tilde{\omega}_n$ determined by

$$\tilde{\omega}_n=\omega_n+i\frac{1}{\hbar}\Sigma(\omega_n)$$

$$=\begin{cases}\omega_n+\dfrac{\Gamma}{\Delta_0}\tilde{\omega}_n\tan^{-1}(\Delta_0/|\hbar\tilde{\omega}_n|) & \text{Axial}\\[2ex]\omega_n+\dfrac{\Gamma}{\Delta_0}\tilde{\omega}_n\log\left(\dfrac{\Delta_0+\sqrt{\Delta_0^2+(\hbar\tilde{\omega}_n)^2}}{|\hbar\tilde{\omega}_n|}\right) & \text{Polar}\end{cases} \quad (3.19)$$

where $\Gamma\equiv\pi N_i N(0)|u|^2$ is a measure of the impurity scattering strength, ω_n is a Matsubara frequency, and $\Delta_0=\Delta_0(T)$ is the gap maximum. When $\Gamma=0$, the frequency sum in (3.17) may be evaluated and we recover (3.4). At finite impurity concentrations, however,

$$\frac{n_{\mu\nu}^p}{n}=3\int_{-\infty}^{\infty}d\xi\int\frac{d\Omega}{4\pi}\hat{k}_\mu\hat{k}_\nu(kT)\sum_n\frac{(\hbar\tilde{\omega}_n)^2-E^2}{((\hbar\tilde{\omega}_n)^2+E^2)^2}, \qquad (3.20)$$

and (3.19) must first be solved self-consistently. We have evaluated (3.20) for axial and polar states following the method of Skalski et al. [27], and obtained analytic expressions for the limiting low-temperature behavior of the eigenvalues $n_\parallel^p$ and $n_\perp^p$. Below we merely state the relevant results; a fuller treatment will be given in a subsequent publication [28].

1. For an axial superconductor in the presence of a small number of impurities, up to a critical concentration defined by $\Gamma/\Delta_0=2/\pi$, we find that the results for a pure system are renormalized in a trivial way. The paramagnetic density takes the following form at low temperatures:

$$\left.\begin{aligned}n_\parallel^p&=3\frac{\Gamma}{\Delta_0}\left(\frac{\pi}{2}\ln 2-1\right)+\pi^2\left(\frac{kT}{\Delta_0}\right)^2\left(1-\frac{\Gamma}{\Delta_0}\frac{\pi}{2}\right)^{-1}\\[1ex]n_\perp^p&=3\frac{\Gamma}{\Delta_0}\left(1-\frac{\pi}{8}-\frac{\pi}{4}\ln 2\right)\\[1ex]&\quad+\frac{7}{15}\pi^4\left(\frac{kT}{\Delta_0}\right)^4\left(1-\frac{\Gamma}{\Delta_0}\frac{\pi}{2}\right)^{-3}\end{aligned}\right\}\begin{aligned}&\text{Axial}\\[1ex]&\frac{\Gamma}{\Delta_0}<\frac{2}{\pi}\end{aligned}$$

$$(3.21)$$

The power-law temperature dependences characterizing the response in the two directions in the plane are thus unchanged, with a modified prefactor which increases with the impurity scattering rate Γ. As in the usual s-wave case (magnetic impurities), a "normal component" to the response is present even at zero temperature; the $T=0$ penetration depth, for example, will always increase with the addition of impurities. Clearly at the critical value $\Gamma/\Delta_0=2/\pi$ the range of validity of the low-temperature expansion vanishes. Above this value, zero-energy excitations from all points on the Fermi surface contrib-

ute to the BCS density of states and the system enters a "gapless" phase. The temperature dependence of *both* eigenvalues of the paramagnetic response then follows a T^2 law similar to the low-T behavior expected in an ordinary superconductor in the extreme gapless ($\Gamma/kT_c \gg 1$) regime [28].

2. In the polar state, on the other hand, the T and T^3 power laws given in (3.10) are destroyed immediately with the addition of infinitesimal quantities of impurities. When the scattering rate becomes comparable to the renormalized order parameter ($\Gamma/\Delta_0 \gtrsim 0.76$), however, a T^2 behavior is once again realized. The fact that the responses of both classes of anisotropic states display, when sufficiently dirty, the same temperature dependences as an ordinary superconductor in the extreme gapless limit should not be surprising. In all cases the transition occurs as the corresponding BCS density of states becomes flat and featureless at low energies.

Finally, we remark that qualitatively similar conclusions should hold for highly anisotropic singlet superconductors in the presence of paramagnetic impurities.

4. Comparison of Theory and Experiment

It is useful to estimate the zero-temperature penetration depth one would expect from BCS theory, neglecting in the first approximation all corrections due to anisotropy in normal state Fermi surface quantities. A first estimate is obtained from the London expression

$$\lambda(0) = \left(\frac{m^* c^2}{4\pi n_s e^2}\right)^{1/2}, \tag{4.1}$$

where $m^* = 192 m_e$ from the specific heat [29], and each U atom is assumed to contribute three electrons to the superfluid particle density n_s at $T = 0$. The result is $\lambda(0) \simeq 4{,}950$ Å.

An alternative expression for $\lambda(0)$ may be derived from the basic results of BCS and Ginzburg-Landau theory for a type-II superconductor, as

$$\lambda(0) = \frac{(\Phi_0 H_{c2}(0))^{1/2}}{\sqrt{24}\,\delta_{sc} T_c \gamma^{1/2}}, \tag{4.2}$$

where Φ_0 is the flux quantum, $H_{c2}(0)$ is the upper critical field at $T = 0$, $\delta_{sc}^{BCS} = 1.76$ is the ratio of the gap at $T = 0$ to the transition temperature T_c, and γT_c is the electronic specific heat at the transition. This expression gives $\lambda(0) \simeq 5{,}200$ Å with the approximate experimental values of $H_{c2}(0) = 10^5$ gauss, $T_c = 0.86$ K and $\gamma = 1.37 \cdot 10^5$ ergs cm^{-3} K^{-2}.

We may therefore expect a low-T penetration depth of a few thousand angstroms, a factor of ten larger than in "ordinary" superconductors such as Sn, Pb, Nb, etc. This is consistent with the rough estimate of 2,000 Å made by MacLaughlin et al. [4] on the basis of NMR data. We have, however, neglected Landau molecular-field corrections, and from the discussion of Sect. 3d it is clear that if the Galilean-invariance effective-mass relation holds approximately in UBe_{13}, this enhancement will not be observed.

The T^2 behavor of the penetration depth observed at low temperatures is inconsistent with the predictions of BCS theory for a pure, weak-coupling singlet isotropic superconductor. As argued above, the temperature dependence can be explained by assuming the existence of a gap with linearly vanishing point nodes located at any point on the Fermi surface except exactly perpendicular to the vector potential $\vec{A}$. If the state is anisotropic the penetration depth observed in a real experiment need not correspond directly to one of the eigenvalues of the superfluid density tensor even for the relatively simple model order parameters discussed above. Nevertheless, at low temperatures we expect a T or a T^2 behavior to dominate, depending on whether the state possesses lines or points of nodes, respectively. The axial state thus represents a possible fit to the experimental data, provided the $\hat{l}$-vector is not fixed exactly perpendicular to the sample surface over a distance large compared to λ. This will always be the case if the magnetic and/or crystal field orienting effects are sufficiently strong.

The presence of impurities can strongly alter the expected characteristic low-temperature power laws. We make no attempt to estimate the residual impurity-scattering rate in our samples since there exists no quantitative theory of the large low-T intrinsic Kondo scattering. In the presence of the relatively large errors in determining sample surface areas and in the absence of an absolute measurement of $\lambda(0)$, a fit of (3.21) to the data does not provide useful new information. On the other hand, the insensitivity of the T^2 power law in $\lambda - \lambda(0)$ for an anisotropic superconductor with point nodes in the presence of small amounts of impurities is important qualitative support for the hypothesis that pairing of this type is responsible for the observed experimental behavior.

Of course, a dirty superconductor of any of the types discussed in Sect. 3e would also display a similar temperature dependence in the electromagnetic response. A naive explanation based on the assumption of gapless (singlet or triplet) superconductivity may be ruled out, however, by the observation of a T^3 temperature dependence of the specific heat and
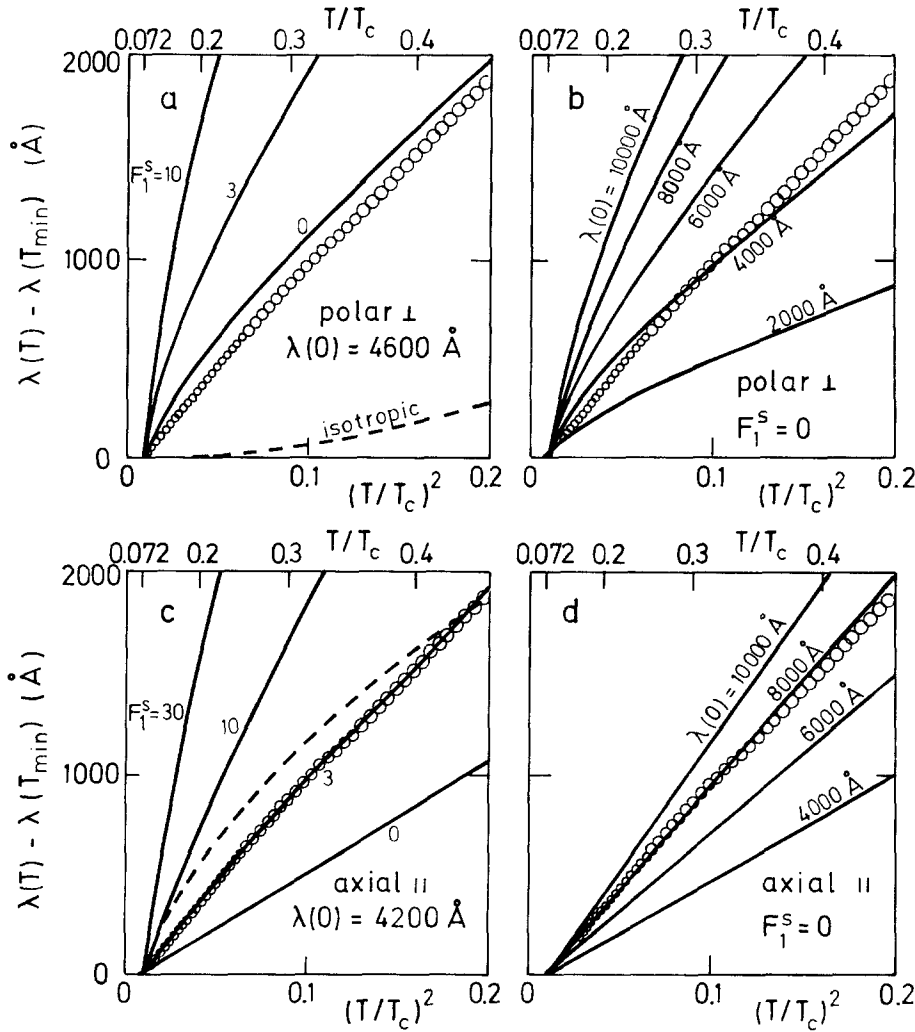
Fig. 7a–d. Comparison of the measured incremental penetration depth $\lambda(T) - \lambda(T_{min})$ (circles), plotted vs. $(T/T_c)^2$, with theory (full and dashed lines). We show polar (a, b) and axial (c, d) gap symmetry and vary the two parameters F_1^s (a, c) and $\lambda(0)$ (b, d) as indicated in the figures. Also shown along with the polar state curves (a) is the result for an isotropic gap (dashed line). In Fig. 7c, the dashed line corresponds to $\lambda(0) = 300$ Å, $F_1^s = 300$. The maximum gap is taken from (3.11), but with the experimental value $\Delta C/C_n = 2.5$ [29]

a large specific-heat discontinuity in other experiments on samples with similar T_c's [3, 29].

It is similarly of interest to place an upper limit on the Landau parameter F_1^s, which also leads to deviations from the low-T power laws. To examine the effects of large F_1^s on λ, we have plotted in Fig. 7 attempts to fit the data with various states, taking $\lambda(0)$ and F_1^s as parameters. We plot the difference of the penetration depth from its value at the minimum reduced temperature $T_{min}/T_c = 0.072$ as a function of T/T_c. In Fig. 7a we plot λ for a polar state, taking $\lambda(0) = 4,600$ Å while varying F_1^s. Also shown as a dashed line is the corresponding result expected for an isotropic superconductor without Fermi-liquid effects. In Fig. 7b we fix $F_1^s = 0$ and vary $\lambda(0)$. The disagreement at low temperatures, where power laws

in T/Δ_0 are expected to dominate, is evident. We therefore conclude that our data cannot be explained with the hypothesis of anisotropic pairing with lines of nodes on the Fermi surface.

In Fig. 7c and d we show the equivalent results for $\lambda_{\parallel}$ in an axial superconductor. While a best fit to the entire range of data is obtained for $\lambda(0) = 4,200$ Å, a fit at low temperatures $T/T_c < 0.3$ is always possible, provided $F_1^s < 20$. Also shown is an unsuccessful attempt to fit the data with large F_1^s; strict application of the Galilean-invariance effective-mass relationship would imply $F_1^s \simeq 600$. We note that the value of $\lambda(0)$ obtained from these fits represents at best a rough upper bound to the true value, since, as discussed in Sect. 3, $\hat{l}$ need not be oriented parallel to $\vec{A}$ throughout the sample. Isotropic BCS,

axial $(\hat{l} \perp \vec{A})$ and polar $(\hat{l} \parallel, \perp \vec{A})$ gaps remain inconsistent with the observed T^2 dependence for all choices of the parameters.

5. Conclusions

Our data on the magnetic penetration depth in UBe_{13} may be explained by the assumption of a gap with point nodes on the Fermi surface, provided the Landau parameter $F_1^s \lesssim 20$. The values of $\lambda(0)$ obtained by fitting the expected penetration depth for a model p-wave axial order parameter, which lie in the range between 4,000 and 8,000 Å, are roughly consistent both with the estimates made above and the indirect NMR measurement of MacLaughlin et al. Clearly an *absolute* measurement of $\lambda(T)$ would provide additional valuable information about the gap anisotropy and the spatial distribution of the gap orbital axes, as well as determining F_1^s more exactly. Preparations for such an experiment are in progress.

It seems extremely unlikely that band-structure or electron-phonon effects can so enhance the effective mass as to explain the specific heat measured in UBe_{13} [29]. Alternatively, the local nature of the f-electrons may so strongly break the translational invariance of the heavy electron system that the Galilean invariance relation becomes totally invalid. The smallness of F_1^s, if substantiated, would then lend strong support to those theories which predict a scaling of m^*/m with F_0^s based on an unrenormalized compressibility.

An interesting possible alternative explanation is the assertion of Alekseevkii et al. [8] that a band of light $(m^* \simeq m_e)$ electrons is present. If these carriers support the Meissner current one may produce values of $\lambda(0) \simeq 5{,}000$ Å by assuming a light electron density of approximately 0.05 electrons per U atom. The presence of a light band would also explain the small value of F_1^s observed, since in this case one would expect the quasiparticles to interact weakly. On the other hand, it is difficult to understand how a highly anisotropic gap could result from a weakly interacting band. Theories of heavy electron superconductivity which assume two-band pairing will have to provide an explanation for the observed T^2 temperature dependence of $\lambda - \lambda(0)$.

Note Added in Proof

It has recently been shown [30, 31] that, in the unitary scattering limit, non-magnetic impurities in anisotropic superconductors lead to "gapless" behaviour in low-T thermodynamic and transport properties even at very small impurity concentrations. In this case one may not be able to distinguish between states with points and lines of nodes on the basis of the observed T^2 dependences of $\lambda(T) - \lambda(T_{min})$.

References

1. See Stewart, G.R.: Rev. Mod. Phys. **56**, 755 (1984), and references therein
2. See Lee, P.A., Rice, T.M., Serene, J.W., Sham, L.J., Wilkins, J.W.: Comm. Solid State Phys. (to be published) and references therein
3. Ott, H.R., Rudigier, H., Rice, T.M., Ueda, K., Fisk, Z., Smith, J.L.: Phys. Rev. Lett. **50**, 159 (1983)
4. MacLaughlin, D.E., Cheng Tien, Clark, W.G., Lan, M.D., Fisk, Z., Smith, J.L., Ott, H.R.: Phys. Rev. Lett. **53**, 1833 (1984)
5. Bishop, D.J., Varma, C.M., Batlogg, B., Bucher, E.: Phys. Rev. Lett. **53**, 1009 (1984)
6. Golding, B., Bishop, D.J., Batlogg, B., Haemerle, W.H., Smith, J.L., Fisk, Z., Ott, H.R.: Phys. Rev. Lett. **55**, 2479 (1985)
7. Maple, M.B., Chen, J.W., Lambert, S.E., Fisk, Z., Smith, J.L., Ott, H.R., Brooks, J.S., Naughton, M.J.: Phys. Rev. Lett. **54**, 477 (1985)
8. Alekseevskii, N.E., Narozhnyi, V.N., Wizhankovskii, V.I., Nikolaev, E.G., Khlybov, E.P.: JETP **40**, 1241 (1984)
9. Leggett, A.J.: Phys. Rev. A**140**, 1869 (1965)
10. Andres, K., Wudl, F., Mc.Whan, D.B., Thomas, G.A., Nalewajck, D., Stevens, A.L.: Phys. Rev. Lett. **45**, 1449 (1980)
11. Tai, P.C.L., Beasley, M.R., Tinkham, M.: Phys. Rev. B**11**, 411 (1975)
12. Balian, R., Werthamer, N.R.: Phys. Rev. **131**, 1553 (1963)
13. Millis, A.: Preprint
14. Combescot, R.: J. Low Temp. Phys. **18**, 537 (1975)
15. Daw El Beit, M.S.: Univ. Sussex Ph.D. Thesis, 1982
16. Ambegaokar, V., DeGennes, P.G., Rainer, D.: Phys. Rev. A**9**, 2676 (1974)
17. For a similar calculation, see Leggett, A.J.: Rev. Mod. Phys. **47**, 331 (1975)
18. Ohkawa, F.J., Fukuyama, H.: J. Phys. Soc. Jpn. **53**, 4345 (1984)
19. Overhauser, A.W., Appel, J.: Phys. Rev. B**31**, 193 (1985)
20. Valls, O.T., Tesanovic, Z.: Phys. Rev. Lett. **53**, 1497 (1984)
21. Pfitzner, M., Wölfle, P.: Phys. Rev. B **33**, 2003 (1986)
22. Bedell, K.S., Quader, K.F.: Phys. Rev. B**32**, 3296 (1985). In general no simple relation between m^*/m and F_1^s can be expected to hold. In Fermi liquid theory as applied by Bedell and Quader, the ratio $m^*/(1 + F_1^s/3)$ defines another mass m_λ, which reduces to the crystalline mass m only in the Galilean-invariant case. Note that in the present work m always refers to the crystalline mass, while m^* contains, in addition interaction effects
23. Varma, C.M.: Phys. Rev. Lett. **55**, 2723 (1985)
24. Rice, T.M., Ueda, K.: Phys. Rev. Lett. **55**, 995 (1985)
25. Ueda, K., Rice, T.M.: In: Proceedings of the 8th Taniguchi Symposium, "Theory of Heavy Fermions and Valence Fluctuations", Kazuya, T. (ed.). Berlin, Heidelberg, New York: Springer 1985
26. Abrikosov, A.A., Gor'kov, L.P.: Sov. Phys. JETP **12**, 1243 (1961)

27. Skalski, S., Betbeder-Matibet, O., Weiss, P.R.: Phys. Rev. **136**, A1500 (1964)
28. Einzel, D., Hirschfeld, P.: (to be published)
29. Ott, H.R., Rudigier, H., Fisk, Z., Smith, J.L.: Phys. Rev. Lett. **50**, 1595 (1983)
30. Hirschfeld, P., Vollhardt, D., Wölfle, P.: Solid State Commun. **59**, 111 (1986)
31. Schmitt-Rink, S., Miyake, K., Varma, C.M.: (to be published)

F. Gross
B.S. Chandrasekhar
D. Einzel
K. Andres
Walther Meissner-Institut
für Tieftemperaturforschung
D-8046 Garching bei München
Federal Republic of Germany

P.J. Hirschfeld
Physik-Department
Technische Universität München
D-8046 Garching bei München
Federal Republic of Germany

H.R. Ott
Laboratorium für Festkörperphysik
Eidgenössische Technische Hochschule
Hönggerberg
CH-8093 Zürich
Switzerland

J. Beuers
Max-Planck-Institut für Metallforschung
Heisenbergstrasse 1
D-7000 Stuttgart 80
Federal Republic of Germany

Z. Fisk
J.L. Smith
Los Alamos National Laboratory
Los Alamos, NM 87545
USA